

Structural Determination of the *O*-Specific Chain of the Lipopolysaccharide Fraction from the Alkaliphilic Bacterium *Halomonas magadii* Strain 21 MI

Cristina de Castro,^[a] Antonio Molinaro,^[a] Andrew Wallace,^[b] William D. Grant,^[b] and Michelangelo Parrilli*^[a]

Dedicated to Professor Lorenzo Mangoni on occasion of his 70th birthday

Keywords: Extremophile / *gulo*-Aminouronic acid / Molecular mechanics / Structure elucidation / Natural products

The complete structure of one of the *O*-specific polysaccharide components from the soda lake bacterium *Halomonas magadii* is described. The structural determination, which was achieved by chemical, spectroscopic, and computational analysis, indicates a novel trisaccharide repeating unit made

up of glucose and two units of 2-acetamido-2-deoxy-guluronic acid: $\rightarrow 4$)- α -L-GulpNAcA-(1 \rightarrow 6)- α -D-Glcp-(1 \rightarrow 4)- α -L-GulpNAcA-(1 \rightarrow (© Wiley-VCH Verlag GmbH & Co. KGaA, 69451 Weinheim, Germany, 2003)

Introduction

Halomonas magadii is a Gram-negative extremophile and alkaliphilic bacterium isolated from Lake Magadi, located in the East African Rift Valley. This lake is in an arid, semi-tropical zone characterised by a surrounding geology high in sodium and low in calcium and magnesium. Evaporation exceeds the rate of inflow of water, producing a high degree of salinity and alkalinity in a number of lakes in the floor of the valley, the most extreme example being Lake Magadi, which is saturated with sodium carbonate and chloride at a pH of around 12. Recently, several members of the halomonad group of bacteria were shown to inhabit the alkaline brines, and these included a new member, *Halomonas magadii* strain 21 MI (NCIMB 13595), an organism that grows at high pH and relatively high salt concentration.^[1] Although *H. magadii* is Gram-negative in nature, nothing is known about the cell wall composition of alkaliphilic halomonads. The structure of the *O*-specific polysaccharide of a component of the LPS fraction of this strain is reported here.

Results and Discussion

Dried cells were extracted by the phenol/water method,^[2] and the LPS fraction was found exclusively in the water

phase; its compositional analysis showed the presence of galactose, glucose, and 2-acetamido-2-deoxy-uronic acid – as shown by their fragmentation patterns^[3] (Figure 1) – as major components, together with mannose, heptose, and KDO as minor ones.

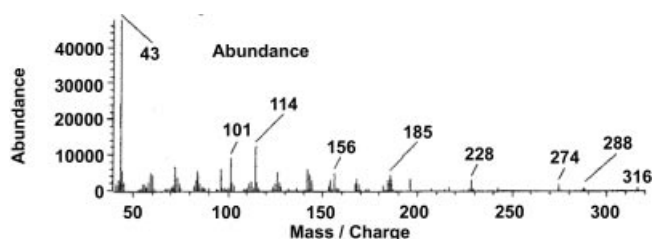


Figure 1. EI-MS spectrum of the acetylated *O*-methyl glycoside methyl ester derivative of *gulo*aminouronic acid; the ions at $m/z = 316$ and 288 are both oxonium cations, the first one deriving from the loss of methoxy group at anomeric position, the second one deriving from the loss of the methoxycarbonyl group at C-5

The isolated LPS material was subjected to vertical gel electrophoresis (Figure 2), and appeared as a complex, disperse, ladder-like pattern, typical of the S-LPS form. The gel showed two different distributions of bands: one at the top of the gel and a second one with a molecular mass distribution similar to that of the reference (*Escherichia coli* O:111). The intensely stained bands dispersed at the bottom of the gel are probably due to the presence of contaminant phospholipids.

The two distributions suggested the presence of two different lipopolysaccharide species, with different average molecular weights.

Two strategies were successfully used to purify the two classes of compounds. The first of these was SEC (Size Ex-

^[a] Dipartimento di Chimica Organica e Biochimica, Università di Napoli "Federico II", Complesso Universitario Monte Sant' Angelo, Via Cintia 4, 80126 Napoli, Italy
Fax. (internat.) +39081674393
E-mail: parrilli@unina.it

^[b] Department of Microbiology and Immunology, University of Leicester, P. O. Box 138, Leicester LE1 9HN, UK

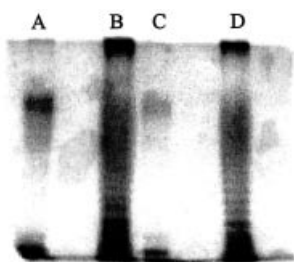


Figure 2. Silver-stained SDS-PAGE electrophoresis of *Halomonas magadii* crude LPS (lanes: B 8 μ g, D 4 μ g) and *E. coli* O111 (lanes: A 8 μ g, C 4 μ g)

clusion Chromatography) under denaturing conditions, performed directly on the LPS mixture,^[4] while the second was isolation of the two *O*-chain moieties after acid hydrolysis of the LPS fraction.

The first approach resulted in the isolation of the two different lipopolysaccharide species: LPS-1 and LPS-2. Compositional analysis and NMR proton spectra (data not shown) suggested that the first LPS fraction was a pure LPS fraction, whereas the second one was still contaminated by small amounts of the former. For this reason, further analyses were focused on the first fraction.

LPS-1 showed good solubility at alkaline pH* values, allowing detailed spectroscopic analysis of the sample (Table 1). Such direct analysis on LPS molecules is not usually feasible, since the hydrophobic lipid A moieties are aggregated in solution, resulting in the formation of micelles. These superstructure exhibit low mobilities in solution, hindering any spectroscopic analysis. The good spectroscopic resolution of this LPS in the present case is probably due to the ionised *O*-chain moiety, promoted by the alkaline pH*; neutral and acidic pH* values were less effective for NMR studies of this sample.

Table 1. ¹H and ¹³C NMR chemical shifts (ppm) of *O*-chain portion measured directly on LPS-1 at pH* 10.6

Sugar residue	1	2	3	4	5	6
6)- α -D-Glcp(1 \rightarrow	5.05	3.51	3.71	3.48	3.80	3.87
A	96.5	72.4	73.5	70.5	71.6	67.9
4)- α -L-GulpNAcA(1 \rightarrow	5.02	4.28	3.98	4.06	4.59	—
B	99.0	47.3	69.0	81.0	67.8	176.2
4)- α -L-GulpNAcA(1 \rightarrow	4.99	4.28	4.17	4.17	4.45	—
C	100.9	47.3	64.9	74.3	67.9	176.0

The ¹H NMR spectrum of the LPS-1 fraction (Figure 3) suggested a regular polysaccharide structure with a trisaccharide repeating unit. ¹³C NMR values (Table 1, from HSQC spectrum) were in agreement with the presence of three pyranose residues: their chemical shifts, together with the information provided by their ¹J_{C,H} constants, as read from a proton-coupled HSQC spectrum, suggested α anomeric configurations for all of them.

The three anomeric proton signals were denoted as A, B and C, according to their decreasing chemical shift values, and complete assignment of all resonances was achieved through detailed 2D NMR analysis (gsCOSY, TOCSY,

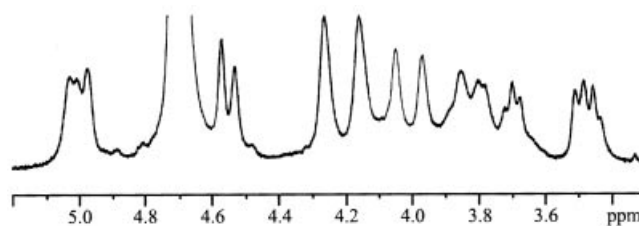


Figure 3. Expanded area of ¹H NMR spectrum at 400 MHz of LPS-1 fraction measured at pH* 10.6

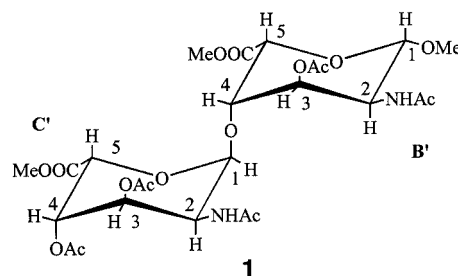
NOESY, gsHSQC, gsHMBC, Table 1). In particular, proton A-1 was scalar coupled to the high-field proton A-2, a broad doublet coupled in turn to the triplet A-3. Proton A-4, although partially hidden by A-2 was visibly a triplet, while protons A-5 and A-6 were too close and their shapes were not clear. The recognition of the residue A proton's multiplicity allowed the *gluco* configuration to be assigned to this spin system. The carbon chemical shift values were in agreement with those of a α -glucose system, the low-field value of its A-6 carbon (δ = 67.9 ppm) indicating that this position was glycosylated.

The D configuration for glucose was determined by comparison of the acetylated (*S*)-2-octyl glycosides derivative with an authentic standard according to the published method.^[5]

The other two residues, B and C, were ascertained to be two 2-acetamido-2-deoxy-hexuronic residues, as shown by their H-5 long-range correlations to carbonyl groups, and also from their C-2 chemical shifts, diagnostic of acetamido substitution. Furthermore, all the protons appeared as broad singlets, suggesting the same relative configuration for both residues. The small values of the coupling values prevented the immediate identification of their stereochemistry.

The sequence of the monosaccharides in the repeating unit was inferred from interresidual NOE data measured by 2D-NOESY. NOE contacts were found between the anomeric proton C-1 and B-4 (strong), B-1 and A-5 (strong), and A-6 (strong); residue A was linked to unit C, but the substitution pattern of the latter was not clear due to overlapping of C-3 and C-4 resonances.

Conclusive information about the stereochemistry of the B and C residues and about the substitution pattern of residue C was obtained by analysis of derivative 1 and the *O*-chain polysaccharide. Product 1 was obtained by LPS methanolysis, followed by acetylation and purification.



Product **1** was a disaccharide made up of two residues of aminouronic acid, the first unit of which — denoted **B'** in analogy with the LPS attribution — was fixed in the α configuration ($^1J_{C1,H1} = 166.3$ Hz) as an *O*-methyl glycoside. The “*gulo*” configuration assignment was established by NMR analysis as follows (Figure 4 and Table 2): on a steric basis, the preferred chair conformation of residue **B'** is the one with the carboxymethyl group in the equatorial orientation and with proton **B'**-5 axial. Consequently, proton **B'**-4 had to be equatorial, as dictated by its small (1.5 Hz) coupling constant with proton **B'**-5. Other information was obtained by analysis of the multiplicity of **B'**-2, which appeared as a complex multiplet due to its coupling with the amide proton ($\delta = 7.32$ ppm, $^3J_{NH,2} = 8.8$ Hz), the anomeric proton ($^3J_{1,2} = 8.8$ Hz) and proton **B'**-3 ($^3J_{2,3} = 3.2$ Hz). The last two values fitted with the axial orientation of **B'**-2 and the equatorial one of **B'**-3. Residue **C'** differed from **B'** in the anomeric configuration, on the basis of both the $^3J_{H1,H2}$ and the $^1J_{H1,C1}$ (174.1 Hz) coupling constants.

Analysis of the *O*-chain polysaccharide (Table 3) completed the data required for the structural determination of this polysaccharide: it was possible to determine the attachment point of residue **C** and to evaluate the NOE contacts necessary for the absolute configuration determination of the two *gulo*aminouronic residues. Unlike the whole LPS, this *O*-chain showed good solubility over a wide range of pH values. Acidic conditions were selected for the analysis conditions, since most of the ring protons were not overlapped in the 1H NMR spectrum (Figure 5), the only exceptions being **B**-1 with **A**-1 and **B**-5 with **C**-5 (Table 3). Never-

Table 3. 1H and ^{13}C NMR spectroscopic data of *O*-chain polysaccharide at $pH^* = 1.0$.

Sugar residue	1	2	3	4	5	6
6)- α -D-Glcp-(1→ A	5.04	3.54	3.67	3.41	3.69	3.97–3.87
4)- α -L-GulpNAcA-(1→ B	98.7	72.4	73.2	71.0	72.8	68.9
4)- α -L-GulpNAcA-(1→ C	5.04	4.32	4.08	4.17	4.94	—
	98.7	47.6	68.5	80.5	67.0	—
	5.13	4.36	4.13	4.25	4.94	—
	100.8	47.1	65.6	76.1	67.0	—

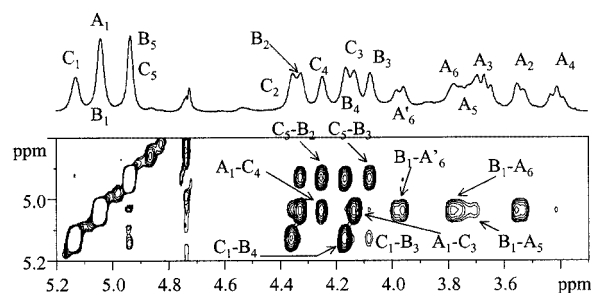


Figure 5. NOESY spectrum expansion and proton projection (400 MHz) of the *O*-chain from *H. magadii* obtained at $pH^* = 1.0$; relevant NOE effects and their attributions are indicated

theless, the spectrum was completely assigned by means of a series of 2D NMR spectra, solving all the ambiguities originating from the NMR spectroscopic data of LPS-1. Through these experiments it was possible to determine the carbon chemical shifts associated with protons **C**-3 ($\delta = 65.6$ ppm) and **C**-4 ($\delta = 76.1$ ppm), position **C**-4 being identified as the one glycosylated on the **C** residue; moreover, the diagnostic NOEs (Table 4 provides a more quantitative estimation of the more relevant ones, while Figure 6 shows a three-dimensional view of the trisaccharide unit) between protons **A**-1 and both **C**-3 (strong) and **C**-4 (medium/strong) were now detected.

In order to relate the NOE pattern to the stereochemistry of the residues involved, molecular mechanic calculations were employed. Specifically, the two **A**–**C** disaccharides α -D-Glc-(1→4)- α -L-GulNAcA (conformational map and geometrical details in Figure 7) and α -D-Glc-(1→4)- α -D-GulNAcA, were built with the MACROMODEL package and subjected to MM3* force-field calculations. Average interproton distances were obtained from the conformational maps of the two simulated disaccharides and translated into expected NOEs, and the NOEs predicted for both cases

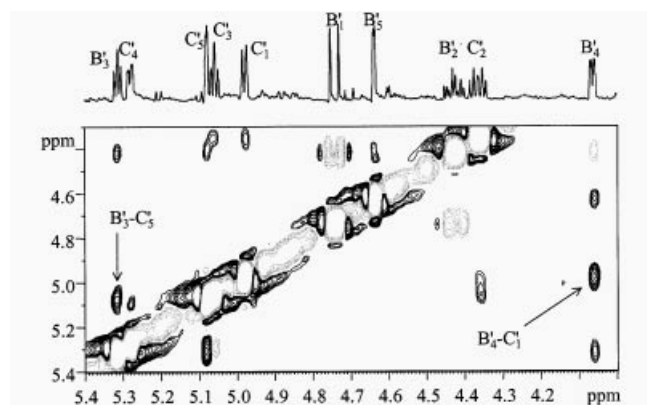


Figure 4. ROESY spectrum expansion and proton projection at 400 MHz of product **1** in $[D_6]$ acetone at 293 K; most of the relevant NOE effects (positive levels, in black) are indicated

Table 2. 1H , $^3J_{H,H}$ (Hz) and ^{13}C (italic) NMR chemical shifts (ppm) of derivative **1** in $[D_6]$ acetone at 293 K.

Sugar residue	1	2	3	4	5
4)- α -L-GulpNAcA-OMe B'	4.74 <i>d</i> $J_{1,2} = 8.8$ 99.2	4.43 <i>dt</i> $J_{2,3} = 3.2$; $J_{NH,2} = 8.8$ 48.7	5.13 <i>t</i> $J_{3,4} = 3.2$ 71.1	4.06 <i>dd</i> $J_{4,5} = 1.5$ 75.3	5.08 <i>d</i> 66.7
α -L-GulpNAcA-(1→ C'	4.98 <i>d</i> $J_{1,2} = 4.3$ 100.3	4.36 <i>dt</i> $J_{2,3} = 4.3$; $J_{NH,2} = 8.9$ 45.4	5.06 <i>t</i> $J_{3,4} = 4.3$ 67.6	5.28 <i>dd</i> $J_{4,5} = 1.2$ 68.3	5.08 <i>d</i> 66.7

Table 4. NOEs observed on *O*-chain (solvent: D₂O, *T* = 313 K, pH* = 1.0); NOEs are expressed as percentages with respect to the diagonal peak of their row

NOE observed			NOE simulated
<i>O</i>-Chain pH* = 1.0 313 K, D ₂ O	A ₁ – C ₄	7.9	7.5
	A ₁ – C ₃	16.0	25.0
	B ₁ – A _{6'}	11.8	[a]
	B ₁ – A ₆	strong ^[b]	[a]
	B ₁ – A ₅	strong ^[b]	[a]
	C ₁ – B ₄	18.0	20.7
	C ₁ – B ₃	2.0	5.0

[a] This dihedral map has not been elaborated. [b] These densities were not suitable for normalization due to partial overlapping of B₁ – A₆ and B₁ – A₅ cross peaks.

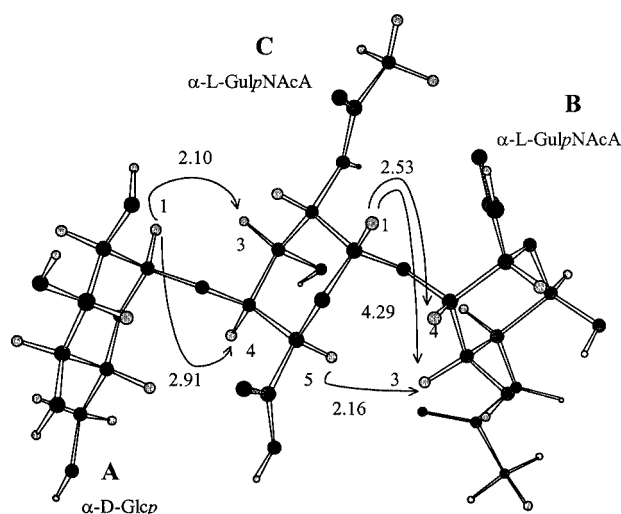


Figure 6. Three-dimensional view of α -D-Glcp-(1 \rightarrow 4)- α -L-GulpNAcA-(1 \rightarrow 4)- α -L-GulpNAcA trisaccharide, more relevant NOE effects are indicated by arrows, together with the distances (in Å) found for the global minimum energy

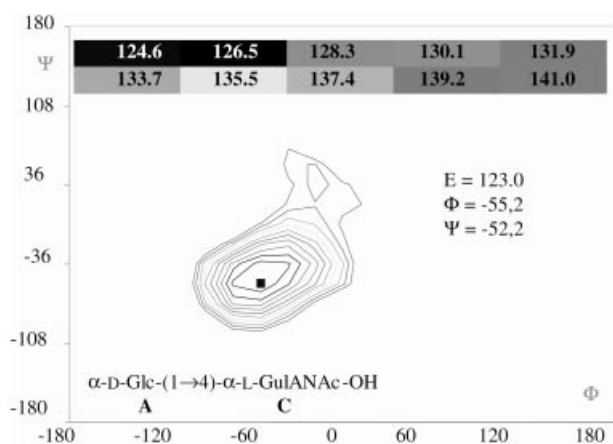


Figure 7. Contour map of the two dihedral angles Φ and Ψ elaborated for disaccharide α -D-Glcp-(1 \rightarrow 4)- α -L-GulpNAcA; energy levels are expressed in kJ/mol and are indicated on the top of the picture, energy minimum values and the corresponding dihedral angles are indicated.

were then compared with those measured experimentally. The only disaccharide fitting with these data was the first one considered, which resulted in the assignment of the L

configuration to the *gulo*aminouronic acid residue **C**. The same approach was adopted to check whether the **C** and **B** residues had the same absolute configuration (conformational map and geometrical details in Figure 8). In this case the experimental NOEs were obtained both from the NOESY spectrum of the *O*-chain and from the ROESY experiment for the derivative **1**: the effects are stronger in the NOESY spectrum than in the ROESY, but in the second case all the proton signals were visible in the spectrum (Figure 4) without any overlapping.

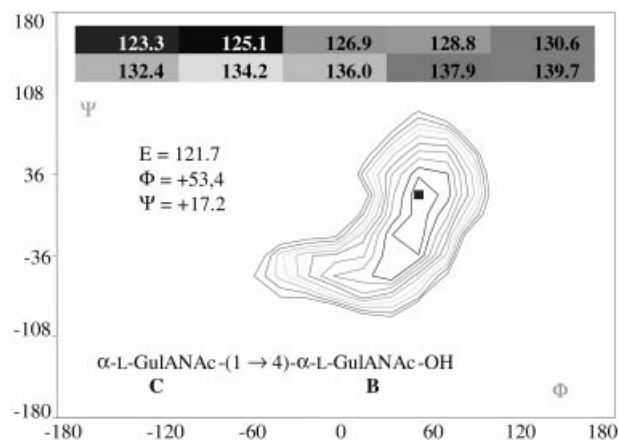


Figure 8. Contour map of the two dihedral angles Φ and Ψ elaborated for disaccharide α -L-GulpNAcA-(1 \rightarrow 4)- α -L-GulpNAcA; energy levels are expressed in kJ/mol and are indicated on the top of the picture, energy minimum values and the corresponding dihedral angles are indicated

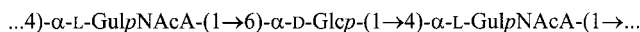
The two analysis converged on the same result, the only disaccharide compatible with the observed NOEs being made up of two L-*gulo*aminouronic residues.

The absolute configuration data were supported by analysis of the ¹³C glycosylation shift values;^[6] by this approach the established rules were applied to the disaccharides α -D-Glc-(1 \rightarrow 4)- α -L-GulpNAcA and α -D-Glc-(1 \rightarrow 4)- α -D-GulpNAcA, and the ¹³C chemical shifts for each residue were compared with those of the unsubstituted glycoside.^[6] In the first case, a downfield shift of 4 ppm was expected for both carbons A-1 and C-4, together with a similar upfield shift for carbon C-3. In the second case, both carbons A-1 and C-4 should experience a larger downfield shift (δ = 8 ppm), together with a very small upfield shift for C-3 signal.^[7] The only combination that matched the experimentally measured data was the first one, supporting the results obtained from the computational analysis for residue **C**.

The reference compound selected for comparison with the ¹³C values of the GulpNAcA residue is residue **C'** in compound **2**, which is obviously not glycosylated.

As for the absolute configuration of the second GulpNAcA residue (**B** unit), the disaccharide fragment α -L-GulpNAcA-(1 \rightarrow 4)-GulpNAcA (**C-B**) was considered. In this case, an L configuration of the **B** residue would imply a larger downfield shift of C-4 and a smaller upfield shift of the C-3 signals of the **B** unit, as was found experimentally (Table 3).

From the above data, the structure of the *O*-chain polysaccharide from LPS-1 is unequivocally determined as shown.



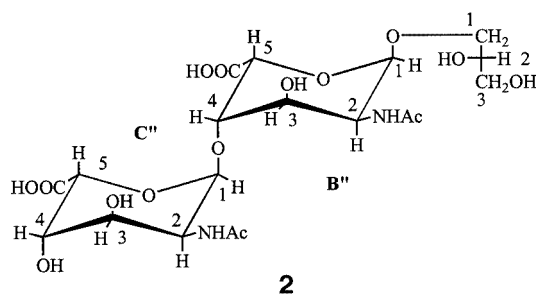
B

A

C

The proposed structure was in agreement with the observed Smith degradation product: compound **2**, a disaccharide glycoside with a 1-substituted glycerol residue as the aglycon moiety. The **C''** unit was the terminal non-reducing residue, and its carbon chemical shift values were assumed as reference for the above considerations (Table 5).

In conclusion, the complete *O*-chain structure of one of the LPSs produced by the alkaliphilic and halophilic bacterium *Halomonas magadii* has been deduced. Interestingly, this is one of the few cases in which spectroscopic analysis could be carried out directly on the intact LPS. The close similarity of the ^1H NMR spectra of this and of the *O*-chain polysaccharide demonstrated that no acid-labile substituents (such as deoxy sugars, phosphates, or acetates) were present on the intact molecule and allowed the application of the standard Kdo linkage acid hydrolysis, used to cleave the *O*-chain from the Lipid A part.

**2**

The anionic nature of this *O*-chain may be an adaptation response of the bacterium to its harsh environment. This organism was isolated from Lake Magadi, which is characterised by extremely high Na_2CO_3 and NaCl concentrations ($>3.5\text{ M}$) and a pH range between 10–12. The *O*-chain may act as a buffering system, able to keep the pH value buffered in the region immediate to the external membrane surface, protecting the bacterium from the aggressive medium.

Experimental Section

Growth of *Halomonas magadii*, Isolation of LPS-1: The *Halomonas magadii* strain was isolated from Lake Magadi, Kenya and cultivated as reported.^[1]

Dried cells (10 g) were extracted by the hot phenol-water method.^[2] Both phases were separately dialysed against distilled water, freeze-dried and screened by discontinuous SDS PAGE (Sodium Dodecyl Sulfate Polyacrylamide Electrophoresis),^[8] with a 12% gel on a miniprotein gel system from Bio-Rad; the samples were run at constant voltage (150 V) and stained by Kittelberger's procedure^[9] (Figure 2): the lipopolysaccharide material was recovered exclusively in the water phase (500 mg, 5% yield).

The LPS fraction (50 mg) was subjected to denaturing chromatography as reported by Severn,^[4] and the eluate was monitored by refractive index (R401 Waters). Two main peaks were collected, extensively dialysed and freeze-dried, to afford LPS-1 (18%) and LPS-2 (72%).

Compositional Analysis of the LPS-1 Fraction: Monosaccharides were analysed by GLC-MS as acetylated *O*-methyl glycoside derivatives and lipids as their methyl ester derivatives, as reported previously.^[10]

Absolute configurations of glucose were established by GLC analysis of acetylated glycoside derivatives of (+)-2-octanol, by the published method.^[5]

GLC-MS was performed on a Hewlett–Packard 5890 instrument, SPB-5 capillary column (0.25 mm \times 30 m, Supelco); for compositional analysis the temperature program was: 150 $^\circ\text{C}$ for 5 min, then 5 $^\circ\text{C min}^{-1}$ to 300 $^\circ\text{C}$, while for absolute configuration analysis it was: 150 $^\circ\text{C}$ for 8 min, then 2 $^\circ\text{C min}^{-1}$ to 200 $^\circ\text{C}$ for 0 min, then 6 $^\circ\text{C min}^{-1}$ to 260 $^\circ\text{C}$ for 5 min.

Methylation analysis was attempted by Sanford's procedure,^[11] but did not produce clear results, probably due to the presence of the GulNAcA residue.

Isolation of the *O*-Specific Polysaccharide Fraction: The following procedure was applied both to LPS-1 and to the crude LPS mixture, resulting in both cases in the isolation of the *O*-chain from LPS-1.

Typically, LPS-1 fraction was dissolved in acetic acid solution (1%, 10 mg/ml) and kept at 100 $^\circ\text{C}$ for 2 h. After cooling, the solution was centrifuged at 6000 rpm for 20 min and the supernatant was freeze-dried. The supernatant was further purified by SEC on Se-

Table 5. ^1H , $^3J_{\text{H,H}}$ (Hz) and ^{13}C (NMR chemical shifts (ppm) of Smith degradation product **2**, at pH* 1.0

Sugar residue	1	2	3	4	5
$\alpha\text{-L-GulpNAcA (1}\rightarrow\text{6)}$ C''	5.11 <i>d</i> $J_{1,2} = 4.2$ 101.5	4.29 <i>t</i> $J_{2,3} = 4.2$ 46.6	3.96 <i>t</i> $J_{3,4} = 4.2$ 69.7	4.23 <i>dd</i> $J_{4,5} = 1.2$ 70.9	4.83 <i>d</i> 68.0
4)- $\alpha\text{-L-GulpNAcA}$ B''	5.02 <i>d</i> $J_{1,2} = 4.2$ 99.9	4.32 <i>t</i> $J_{2,3} = 4.2$ 47.5	4.06 <i>dd</i> $J_{3,4} = 4.2$ 68.7	4.15 <i>dd</i> $J_{4,5} = 1.1$ 80.9	4.89 <i>d</i> 67.2
1-linked glycerol	3.54 <i>dd</i> – 3.86 <i>dd</i> $J_{1,2} = 3.4$, $J_{1',2} = 7.0\text{ Hz}$, $J_{1,1'} = 10.9$ 72.2	3.94 <i>m</i> 72.0	3.58 <i>dd</i> – 3.65 <i>dd</i> $J_{3,2} = 4.8$, $J_{3',2} = 5.2\text{ Hz}$, $J_{3,3'} = 10.9$ 64.0		

phacryl HR 300 (Pharmacia, 1.5×70 cm, NH_4HCO_3 50 mM, flow 0.4 mL/min), and the eluate was monitored by refractive index as described above. The *O*-chain was recovered in 75% yield from LPS-1.

Preparation of Product 1: Crude LPS (20 mg) was methanolysed (1 M HCl, 80 °C, 10 h) and acetylated as previously reported.^[10] The methyl glycoside mixture was separated by preparative TLC (Thin Layer Chromatography), eluting with 4:1 benzene/ethanol. NMR analysis, in $[\text{D}_6]\text{acetone}$ at 293 K (Table 2), revealed that the lower spot on TLC ($R_F = 0.13$, 10% yield) was the disaccharide **1**, composed of two units of *gulo*aminouronic acid: the reducing end was blocked as α -methyl glycoside, both carboxylic functions were esterified, and the free hydroxyl residues were acetylated.

Preparation of Product 2. Smith Degradation: Product **2** was obtained by Smith degradation:^[12] briefly, LPS-1 was treated with NaIO_4 (50 mM) at 4 °C for 3 days, followed by addition of ethane-1,2-diol, reduction (NaBH_4), acidification (2 M acetic acid), dialysis and freeze-drying. The oxidised polymer was then hydrolysed with 1% acetic acid at 100 °C, 1.5 h, and acid was removed by freeze-drying. The product was purified by Bio-Gel P2 (2×100 cm), eluted with 50 mM ammonium hydrogen carbonate buffer (pH, 5), monitored with a Waters differential refractometer, and dried (50% yield from LPS-1).

Molecular Mechanics Calculations: Molecular mechanics calculations were performed with the MM3* force-field as implemented in MACROMODEL 7.2, installed under the Red Hat 7.2 operative system. The MM3* force-field^[13] used differs from the regular MM3 force-field in the treatment of the electrostatic term, since it uses charge-charge instead of dipole-dipole interactions. For every glycosidic linkage, Φ is defined as $\text{H}_1-\text{C}_1-\text{O}-\text{C}_{\text{aglycon}}$ and Ψ as $\text{C}_1-\text{O}-\text{C}_{\text{aglycon}}-\text{H}_{\text{aglycon}}$. Both *D* and *L* configurations were considered for residues **B** and **C**, while the *D* configuration was set for glucose residue **A**. Therefore, the following four disaccharide entities were considered: α -D-Glcp-(1 \rightarrow 4)- α -L-GulpNAcA, α -D-Glcp-(1 \rightarrow 4)- α -D-GulpNAcA, α -L-GulpNAcA-(1 \rightarrow 4)- α -L-GulpNAcA and α -L-GulpNAcA-(1 \rightarrow 4)- α -D-GulpNAcA. The calculations were performed for a dielectric constant $\epsilon = 80$, as an approximation for bulk water. Energy maps were calculated for the constituent isolated disaccharides, by employing the DRIV utility (with the DEBG option 150 of the program^[14]) and adiabatic surfaces were visualised with the 2D-plot facility. In the DRIV option, both Φ and Ψ were varied incrementally by use of a grid step of 18°, each (Φ , Ψ) point of the map was optimised by a 1000 P.R. conjugate gradient.^[15]

Probability distributions were calculated for each ϕ , ψ point according to a Boltzmann function as follows: at 313 K for both **A**–**C** and **C**–**B** disaccharides, at 293 K for disaccharide **C**–**B** derivative **1**. Ensemble-average distances and NOEs between intra- and interresidue proton pairs were calculated as reported.^[10]

NMR Spectroscopy: NMR experiments were carried out on a Bruker DRX 400 MHz machine equipped with reverse multinu-

clear probe at 313 K, or at 293 K when in $[\text{D}_6]\text{acetone}$. Chemical shifts of spectra recorded in D_2O are expressed in δ relative to internal acetone (2.225 and 31.4 ppm), whereas spectra in $[\text{D}_6]\text{acetone}$ are referred to the chemical shifts of the solvent; the pH^* solution was measured by calibrating the electrode with standard buffers and without correcting the resulting value for the deuterium isotopic effect. Two-dimensional spectra (gsCOSY, phase-sensitive TOCSY, ROESY and NOESY, and phase-sensitive gradient-HSQC) were measured by use of standard Bruker software.

For homonuclear experiments, typically 512 FIDs of 1024 complex data points were collected, with 40 scans per FID. In all cases, the spectral width was set to 10 ppm and the carrier was placed at the residual HOD peak. A mixing time of 200 ms was used for both NOESY and ROESY experiments. For the HSQC spectrum, 256 FIDS of 1024 complex points were acquired with 50 scans per FID, the GARP sequence being used for ^{13}C decoupling during acquisition. Processing and plotting was performed by use of the standard Bruker XWin NMR 1.3 program.

Acknowledgments

We thank the Centro di Metodologie Chimico-Fisiche of the University Federico II of Naples for the NMR spectra.

- [1] A. W. Duckworth, W. D. Grant, B. E. Jones, D. Mejer, M. C. Marequez, A. Ventosa, *Extremophiles* **2000**, *4*, 53–60.
- [2] O. Westphal, K. Jann, *Meth. Carbohydr. Chem.* **1965**, *5*, 83–91.
- [3] J. Lonngrén, S. Svensson, *Adv. Carbohydr. Chem. Biochem.* **1974**, *29*, 41–106.
- [4] W. B. Severn, A. M. Jones, G. W. Kittelberger, G. W. de Lisle, P. H. Atkinson, *J. Microbiol. Meth.* **1997**, *28*, 123–130.
- [5] K. Leontein, B. Lindberg, J. Lonngrén, *Carbohydr. Res.* **1978**, *62*, 359–362.
- [6] G. M. Lipkind, A. S. Shashkov, Y. A. Knirel, E. V. Vinogradov, N. K. Kochetkov, *Carbohydr. Res.* **1988**, *175*, 59–75.
- [7] A. S. Shashkov, G. M. Lipkind, Y. A. Knirel, N. K. Kochetkov, *Magn. Reson. Chem.* **1988**, *26*, 735–747.
- [8] U. K. Laemmli, *Nature* **1970**, *97*, 620–628.
- [9] R. Kittelberger, F. Hilbink, *J. Biochem. Biophys. Meth.* **1993**, *26*, 81–86.
- [10] J. Jimenez-Barbero, C. De Castro, A. Evidente, A. Molinaro, M. Parrilli, G. Surico, *Eur. J. Org. Chem.* **2002**, *11*, 1770–1775.
- [11] P. A. Sandford, H. E. Conrad, *Biochemistry* **1966**, *5*, 1508–1517.
- [12] F. Smith, R. Montgomery, *Methods Biochem. Anal.* **1956**, *3*, 153–XXXX.
- [13] N. L. Allinger, Y. H. Yuh, J. H. Lii, *J. Am. Chem. Soc.* **1989**, *111*, 8551–8566.
- [14] With DEBG 150, the DRIV option starts each incremental minimisation from the initial structure as read from the input.dat file.
- [15] E. Polak, G. Ribiere, *Revue Francaise Inf. Rech. Oper.* **1969**, *16-R1*, 35.

Received June 18, 2002
[O02336]